Biochemistry

pubs.acs.org/biochemistry Article

The Organization of Active Site Side Chains of Glycerol-3-phosphate Dehydrogenase Promotes Efficient Enzyme Catalysis and Rescue of Variant Enzymes

Judith R. Cristobal, Archie C. Reyes, and John P. Richard*

Cite This: *Biochemistry* 2020, 59, 1582−1591 Read Online

ACCESS | Metrics & More | Article Recommendations

ABSTRACT: A comparison of the values of k_{cat}/K_m for reduction of dihydroxyacetone phosphate (DHAP) by NADH catalyzed by wild type and K120A/R269A variant glycerol-3-phosphate dehydrogenase from human liver (*hl*GPDH) shows that the transition state for enzyme-catalyzed hydride transfer is stabilized by 12.0 kcal/mol by interactions with the cationic K120 and R269 side chains. The transition state for the K120A/R269A variant-catalyzed reduction of DHAP is stabilized by 1.0 and 3.8 kcal/mol for reactions in the presence of 1.0 M $EtNH_3^+$ and guanidinium cation (Gua^+), respectively, and by 7.5 kcal/mol for reactions in the presence of a mixture of each cation at 1.0 M, so that the transition state stabilization by the ternary $E{\cdot}EtNH_3^+{\cdot}Gua^+$ complex is 2.8 kcal/mol greater than the sum of stabilization by the respective binary complexes. This shows that there is cooperativity between the paired activators in transition state stabilization. The effective molarities (EMs) of ∼50 M determined for the K120A and R269A side chains are $\ll 10^6$ M, the EM for entropically controlled reactions. The unusually efficient rescue of the activity of *hl*GPDH-catalyzed reactions by the HP_i/Gua^+ pair and by the $Gua^+/EtNH_3^+$ activator pair is due to stabilizing interactions between the protein and the activator pieces that organize the K120 and R269 side chains at the active site. This "preorganization" of side chains promotes effective catalysis by *hl*GPDH and many other enzymes. The role of the highly conserved network of side chains, which include Q295, R269, N270, N205, T264, K204, D260, and K120, in catalysis is discussed.

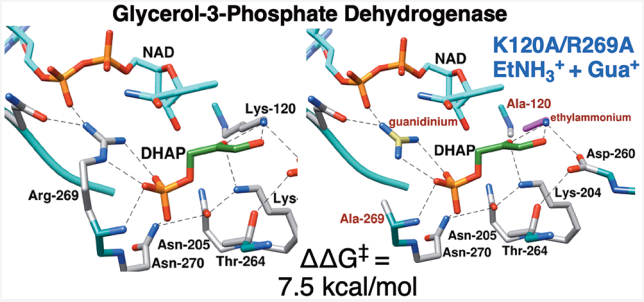

There are many examples of the rescue of the activity of truncated variant enzymes and of truncated alternative substrates by small molecule analogues of the deleted enzyme or substrate piece.[1−9] However, such rescue is not universally observed, and there has been relatively little consideration of the structural requirements for the observation of efficient small molecule rescue of the catalytic activity of truncated enzymes and substrates. These studies provide insight into the mechanism for small molecule activation of enzyme activity that is analogous to allosteric activation, while enabling practical uses of chemical rescue in the activation of enzymes for catalysis.[1,10] A parameter that reports on the efficiency of chemical rescue is the effective molarity (EM) of the truncated amino acid side chain,[11,12] which is calculated as the ratio of k_{cat}/K_m for the wild type enzyme-catalyzed reaction and k'_{cat}/K_dK_X for the reaction catalyzed by the variant enzyme with the missing enzyme piece X, at a standard state of 1 M. The entropic advantage to reaction of the whole enzyme compared to the enzyme in pieces is $\approx 10^6$.[13,14] The EMs of $\ll 10^6$ that we have reported for rescue of variant enzyme-catalyzed reactions are consistent with an attenuation of the entropically controlled EM due to stabilization of the complex with the missing piece by interactions with the protein catalyst.[3,12,15,16]

Glycerol-3-phosphate dehydrogenase (GPDH) catalyzes the reduction of dihydroxyacetone phosphate (DHAP) by NADH to form L-glycerol 3-phosphate [G3P (Scheme 1A)].[17−20] We have examined the activation of wild type human liver GPDH-catalyzed (*hl*GPDH) reduction of glycolaldehyde (GA) by phosphite dianion (HP_i) and determined an EM value of 290 M for the phosphodianion of DHAP at the Michaelis complex with the wild type enzyme.[3,4] The R269 side chain of *hl*GPDH interacts with the phosphodianion of DHAP and provides a 9.1 kcal/mol stabilization of the hydride transfer transition state (Figure 1).[16] We determined an EM value of 60 M for this side chain in a study of the rescue of the R269A variant by the guanidine cation (Gua^+).[16] We next examined the activity of

Received: March 2, 2020
Revised: April 4, 2020
Published: April 6, 2020

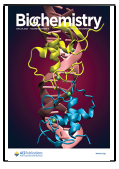

https://dx.doi.org/10.1021/acs.biochem.0c00175
Biochemistry 2020, 59, 1582−1591

Scheme 1. Reactions Catalyzed by (A) Wild Type *hl*GPDH and by (B) R269A and (C) K120A/R269A Variants of the Wild Type Enzyme

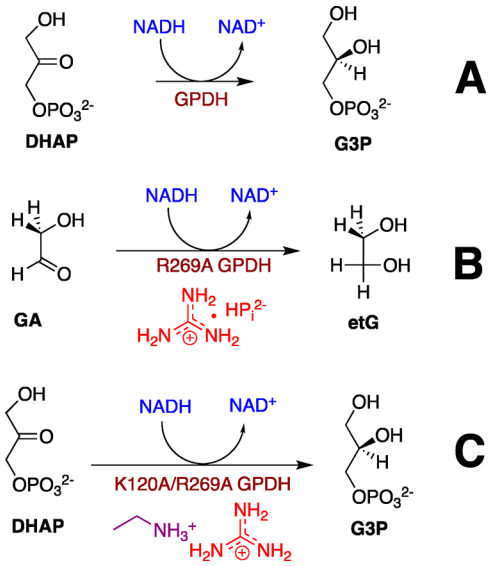

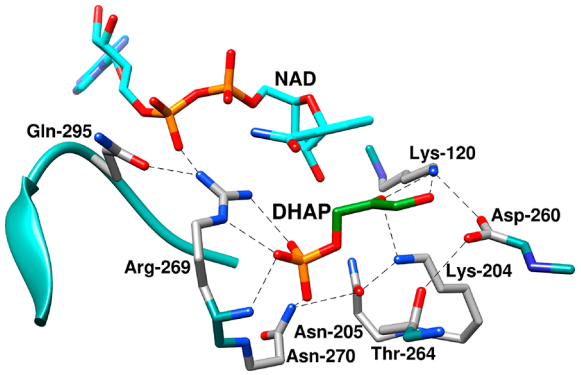

Figure 1. Representation of the X-ray crystal structure of the nonproductive ternary complex of *hl*GPDH, DHAP, and NAD (PDB entry 6E90), which shows the following highly conserved amino acid side chains:[23,24] the side chains of R269 and N270 that interact with the substrate phosphodianion; the side chain of Q295, from a flexible enzyme loop, which interacts with R269; the cationic side chains from K120 and K204; and the side chains from N205, T264, and D260, which are part of a network of hydrogen-bonded side chains that connect the catalytic and dianion activation sites of *hl*GPDH.[25]

the R269A variant toward catalysis of reduction of the truncated substrate GA and characterized the assembly of GA, NADH, Gua^+, HP_i, and the variant enzyme into an active catalyst of reduction of GA (Scheme 1B).[3] These data gave an EM^2 value of 13500 M^2 for the substrate phosphodianion and R269 side chain at the Michaelis complex of DHAP with wild-type *hl*GPDH.

The side chain cation of K120 is positioned to stabilize the negative charge that develops at the C-2 oxygen of DHAP in the transition state for hydride transfer (Figure 1). The loss of this interaction for the K120A variant results in a 5.3 kcal/mol increase in the barrier to reduction of DHAP by NADH, while the loss of the K120 and R269 side chain cation interactions in the K120A/R269A variant results in a 12 kcal/mol barrier increase.[21] These data are consistent with the conclusion that the focused transition state stabilization by the K120 and R269 side chain cations is responsible for a large fraction of the ∼15 kcal/mol stabilization of the hydride transfer transition state.[21,22] The K120 and R269 side chains are part of a network of highly conserved amino acid side chains that extend from Q295 to K120 and that includes N270, N205, K204, T264, D260, and K120 (Figure 1).[23,24] The importance of this network is highlighted by the large effects of N270A[25] and D260G[21] substitutions on the activity of wild type GPDH, but the network's full role in catalysis of hydride transfer has not been determined.

We report here the results of characterization of the efficiency of the rescue of K120A/R269A variant-catalyzed reduction of DHAP by the combined action of Gua^+ and ethylammonium ($EtNH_3^+$) cations (Scheme 1C) and the reduction of GA by the combined action of the phosphite dianion, Gua^+, and $EtNH_3^+$. The first set of experiments shows the efficient rescue by these two cations and gave an EM^2 value of 2400 M^2 for the product of the effective molarity of the K120 and R269 side chains at the wild type enzyme. We conclude that the K120A/R269A variant provides a good template for binding of the excised cationic enzyme pieces and for organization of the K120A and R269A side chains at the active site of wild type *hl*GPDH. By contrast, we did not detect the fifth-order K120A/R269A variant-catalyzed reduction of GA in the presence of HP_i, Gua^+, and $EtNH_3^+$ activators. This sets a limit on the capacity of *hl*GPDH to usefully assemble small molecule activators at the enzyme active site.

EXPERIMENTAL SECTION

Materials. Water was obtained from a Milli-Q Academic purification system. Q-Sepharose and Sephacryl S-200 were purchased from GE Healthcare. Nicotinamide adenine dinucleotide, reduced form (NADH, disodium salt), glycolaldehyde dimer, 2-(*N*-morpholino)ethanesulfonic acid sodium salt (MES, ≥99.5%), triethanolamine hydrochloride (≥99.5%), guanidinium chloride, and sodium phosphite dibasic pentahydrate were purchased from Sigma-Aldrich. Ethylammonium chloride, D,L-dithiothreitol (DTT), sodium hydroxide (1.0 N), and hydrochloric acid (1.0 N) were purchased from Fisher Scientific. All other chemicals were reagent grade or better and were used without further purification. The solution pH was determined at 25 °C using an Orion model 720A pH meter equipped with a Radiometer pHC4006-9 combination electrode that was standardized at pH 4.00, 7.00, and 10.00 at 25 °C. Stock solutions of NADH were prepared by dissolving the disodium form of the coenzyme in water and then stored at 4 °C. The concentration of NADH in these solutions was determined from the absorbance at 340 nm using the extinction coefficient ε of 6220 M^{-1} cm^{-1}. Stock solutions of DHAP were prepared by dissolving the lithium salt of DHAP in water, adjusting the pH to 7.5 with 1.0 NaOH, and storing the solution at −20 °C. The concentration of DHAP was determined as the concentration of NADH consumed during an *hl*GPDH-catalyzed reduction. Published procedures were used to prepare stock solutions of the guanidine cation,[3] ethylammonium cation,[15] and phosphite dianion[6] at pH 7.5. Triethanolamine (TEA) buffers were prepared by addition of 1 M NaOH or 1 M HCl and solid NaCl to give the desired acid/base ratio and final ionic strength. Stock solutions of glycolaldehyde dimer (200 mM monomer) were prepared by dissolving the dimer in water and waiting for 3 days at room temperature to allow for quantitative breakdown of the dimer to the monomer.[6]

https://dx.doi.org/10.1021/acs.biochem.0c00175
Biochemistry 2020, 59, 1582−1591

The K120A/Q295A and K120A/R269A variants of *hl*GPDH were expressed and purified by published procedures.[21] Concentrated solutions of these variants were dialyzed exhaustively against 20 mM TEA buffer (pH 7.5) at 4 °C. When necessary, these solutions were diluted with 20 mM TEA buffer (pH 7.5) that contained 10 mM DTT and 0.1 mg/mL bovine serum alumin (BSA). The concentration of these enzyme variants was calculated from the absorbance at 280 nm using the extinction coefficient ε of 18450 M^{-1} cm^{-1} and a subunit molecular mass of 37500 Da that were determined using the ProtParam tool available on the ExPASy server.[26,27]

Enzyme Assays. All enzyme assays were conducted at an ionic strength I of 0.12 (NaCl) in a volume of 1.0 mL at 25 °C. *hl*GPDH was assayed by monitoring the oxidation of NADH (0.2 mM) by DHAP. Initial velocities of NADH oxidation over ≤10% reaction of DHAP were calculated from the change in absorbance at 340 nm using a molar extinction coefficient of 6220 M^{-1} cm^{-1} for NADH. Published procedures were used to assay the activity of K120A/Q295A and K120A/R269A variant-catalyzed reduction of DHAP by NADH at 25 °C, pH 7.5 (20 mM TEA), and I = 0.12 (NaCl) and for the K120A/R269A variant-catalyzed reduction of GA under the same conditions.[3,21,28]

Activation of Variant *hl*GPDH-Catalyzed Reactions. (A) *Ethylammonium Cation.* The assay mixtures at 25 °C and pH 7.5 (20 mM TEA) contained 0.1 mg/mL BSA and 0.2 mM NADH. For the K120A/Q295A variant, the assay mixture contained 1−3 mM DHAP, 0−80 mM activator, and 2.1 μM K120A/Q295A variant *hl*GPDH. For the K120A/R269A variant, the reaction mixture contained 0.800 mM DHAP and 22 μM K120A/R269A variant *hl*GPDH. The reactions were monitored for 20 min for the K120A/Q295A variant and for 720 min for the K120A/R269A variant.

(B) *Guanidinium Cation.* The assay mixtures at 25 °C and pH 7.5 (20 mM TEA) contained 0.1 mg/mL BSA, 0.2 mM NADH, 0.4−0.8 mM DHAP, 0−60 mM activator, and 20 μM K120A/R269A variant. The initial velocities for oxidation of NADH were calculated from the change in absorbance at 340 nm for a 20−40 min reaction time.

Activation of the K120A/R269A Variant by Mixtures of Guanidinium and Ethylammonium Cations. The assay mixtures for the K120A/R269A variant-catalyzed reduction of DHAP by NADH at I = 0.12 (NaCl) and 25 °C in the presence of mixtures of guanidinium and ethylammonium ions contained 20 mM TEA buffer (pH 7.5), 0.1 mg/mL BSA, 0.2 mM NADH, 0.4−0.8 mM DHAP, 0−60 mM guanidinium and ethylammonium cation activators (total concentration of the mixture), and 20 μM K120A/R269A variant *hl*GPDH. The initial velocities for oxidation of NADH were calculated from the change in absorbance at 340 nm for a 20 min reaction time.

RESULTS

Slow GPDH-catalyzed reactions may be monitored for at least 24 h, during which time there is no detectable (<10%) loss of the activity of the wild type or K120A/R269A variant enzyme. There was no detectable reduction of 1.8 mM GA in the presence of 0.2 mM NADH catalyzed by 30 μM K120A/R269A variant *hl*GPDH (ΔA_{340} < 0.004 for a 40−60 min reaction time). This sets a limit for k_{cat}/K_m of ≤0.003 M^{-1} s^{-1} for this enzymatic reaction.[3] There was likewise no detectable reduction of 1.8 mM GA at 0.2 mM NADH catalyzed by 30 μM K120A/R269A variant *hl*GPDH in the presence of single activator HP_i (20 mM), Gua^+ (20 mM), or $EtNH_3^+$ (20 mM), and in the presence of a mixture of 20 mM HP_i, 20 mM Gua^+, and 20 mM $EtNH_3^+$. There is no detectable effect (<5%) of 60 mM Gua^+ or 60 mM $EtNH_3^+$ on $v/[E]$ for reduction of DHAP by 0.2 mM NADH catalyzed by the K120A or R269A variant, respectively, so that small molecule rescue of these variant enzymes is specific for the cation analogue of the excised side chain.[16,21]

Figure 2 shows plots of $v/[E]$ against [DHAP], with slopes $(k_{cat}/K_m)_{obs}$, for K120A/Q295A *hl*GPDH-catalyzed reduction

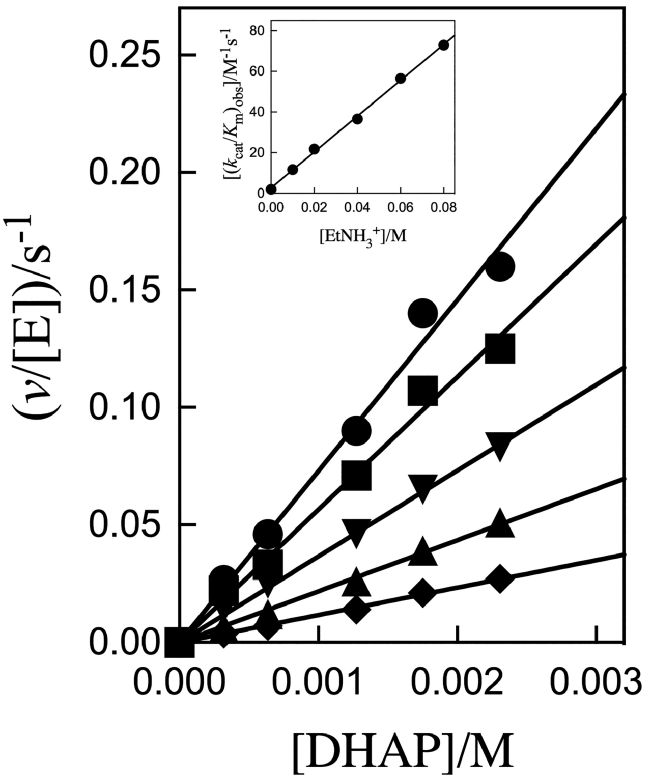

Figure 2. Effect of increasing $[EtNH_3^+]$ on $v/[E]$ (s^{-1}) for K120A/Q295A variant *hl*GPDH-catalyzed reduction of DHAP by NADH for reactions at pH 7.5 (20 mM TEA buffer), 25 °C, saturating [NADH] = 0.2 mM, and I = 0.12 (NaCl): (●) 80 mM cation, (■) 60 mM cation, (▼) 40 mM cation, (▲) 20 mM cation, and (◆) 10 mM cation. The inset shows the plot of $(k_{cat}/K_m)_{obs}$ against $[EtNH_3^+]$, where $(k_{cat}/K_m)_{obs}$ values are the slopes of the correlations from the main panel.

of DHAP by 0.2 mM NADH (saturating)[21] at different fixed $EtNH_3^+$ concentrations. The inset of Figure 2 shows the plot of $(k_{cat}/K_m)_{obs}$ against $[EtNH_3^+]$, with slope k_{cat}/K_mK_{am} of 880 ± 20 M^{-2} s^{-1} (Table 1), for rescue by $EtNH_3^+$. Figure 3A shows the plot of $v/[E]$ against $[EtNH_3^+]$, with slope $(k_{cat}/K_{am})_{obs}$, for K120A/R269A *hl*GPDH-catalyzed reduction of 0.8 mM DHAP by 0.2 mM NADH (saturating).[21] Combining the slope of this correlation $(k_{cat}/K_{am})_{obs}$ (2.8×10^{-5} M^{-1} s^{-1}) with a [DHAP] of 8×10^{-4} M gives a k_{cat}/K_mK_{am} value of 0.035 M^{-2} s^{-1} (Table 1) for rescue of the K120A/R269A variant by $EtNH_3^+$. Figure 3B shows the related plots of $v/[E]$ against $[Gua^+]$, with slopes $(k_{cat}/K_{Gua})_{obs}$, for K120A/R269A *hl*GPDH-catalyzed reduction of 0.8 or 0.4 mM DHAP by 0.2 mM NADH. The inset of Figure 3B shows the plot of $(k_{cat}/K_{Gua})_{obs}$ against [DHAP], with a slope k_{cat}/K_mK_{Gua} of 3.9 ± 0.1 M^{-2} s^{-1} (Table 1) for rescue of the K120A/R269A variant by Gua^+ (Table 1).

https://dx.doi.org/10.1021/acs.biochem.0c00175
Biochemistry 2020, 59, 1582−1591

Table 1. Kinetic Parameters and Derived Gibbs Free Energy Terms for Reactions of the Substrate and Pieces Catalyzed by *hl*GPDH at 25 °C, pH 7.5 (20 mM TEA), and I = 0.12 (NaCl)

For Wild Type *hl*GPDH, k_{cat}/K_m = (4.6 ± 0.3) × 10^6 M^{-1} s^{-1};[a] for Q295A *hl*GPDH, k_{cat}/K_m = (6.3 ± 1.0) × 10^4 M^{-1} s^{-1}[b]

variant	k_{cat}/K_m (M^{-1} s^{-1})[c]	activator	k_{cat}/K_mK_X (M^{-2} s^{-1})[d]	$\Delta\Delta G^{\ddagger}$[e] (kcal/mol)	$\Delta G^{\ddagger}_{Act}$[f] ($\Delta G^{\ddagger}_{Act}/\Delta\Delta G^{\ddagger}$) (kcal/mol)	$\Delta G^{\ddagger}_{S}$[g] (kcal/mol) (EM)[h]
K120A	550 ± 30	$EtNH_3^+$	(8.5 ± 0.4) × 10^4	5.3 ± 0.1	3.0 ± 0.1 (0.57)	2.3 (50 M)
K120A/Q295A	2.0 ± 0.1	$EtNH_3^+$	880 ± 20	6.2 ± 0.1[i]	3.6 ± 0.1 (0.58)	2.5 (70 M)
R269A	1.0 ± 0.2	Gua^+	(8.0 ± 0.5) × 10^4	9.1 ± 0.1	6.7 ± 0.1 (0.74)	2.4 (60 M)
K120A/R269A	(6.2 ± 0.4) × 10^{-3}	$EtNH_3^+$	(3.5 ± 0.4) × 10^{-2}	2.9 ± 0.1[j]	1.0 ± 0.1[l] (0.33)	2.0 (30 M)
		Gua^+	3.9 ± 0.1	6.7 ± 0.1[k]	3.8 ± 0.1[m] (0.56)	2.9 (140 M)
		$EtNH_3^+$·Gua^+	(1.9 ± 0.1) × 10^3 M^{-3} s^{-1}	12.0 ± 0.1	7.5 ± 0.1[n] (0.62)	4.6[o] (2400 M^2)

[a]From ref 4. [b]From ref 28. [c]Second-order rate constant for variant *hl*GPDH-catalyzed reduction of DHAP. [d]Third- or fourth-order rate constant for rescue of the activity of variant enzyme-catalyzed reduction of DHAP by the given activator(s). [e]Effect of the amino acid substitution on the stability of the transition state for wild type *hl*GPDH-catalyzed reduction of DHAP, unless stated otherwise. [f]Effect of 1.0 M activator on the stability of the transition state for the variant *hl*GPDH-catalyzed reaction.[3] [g]Transition stabilization obtained from the covalent connection between the enzyme pieces ($\Delta G^{\ddagger}_S = \Delta\Delta G^{\ddagger} - \Delta G^{\ddagger}_{Act}$). [h]Effective molarity, of wild type or variant *hl*GPDH, of the deleted amino acid side chain [$(k_{cat}/K_m)/k_{cat}/K_mK_X$]. [i]Effect of the K120A substitution on Q295A *hl*GPDH. [j]Effect of the K120A substitution on R269A *hl*GPDH. [k]Effect of the R269A substitution on K120 *hl*GPDH. [l]Using eq 6. [m]Using eq 7. [n]Using eq 3. [o]Using eq 5.

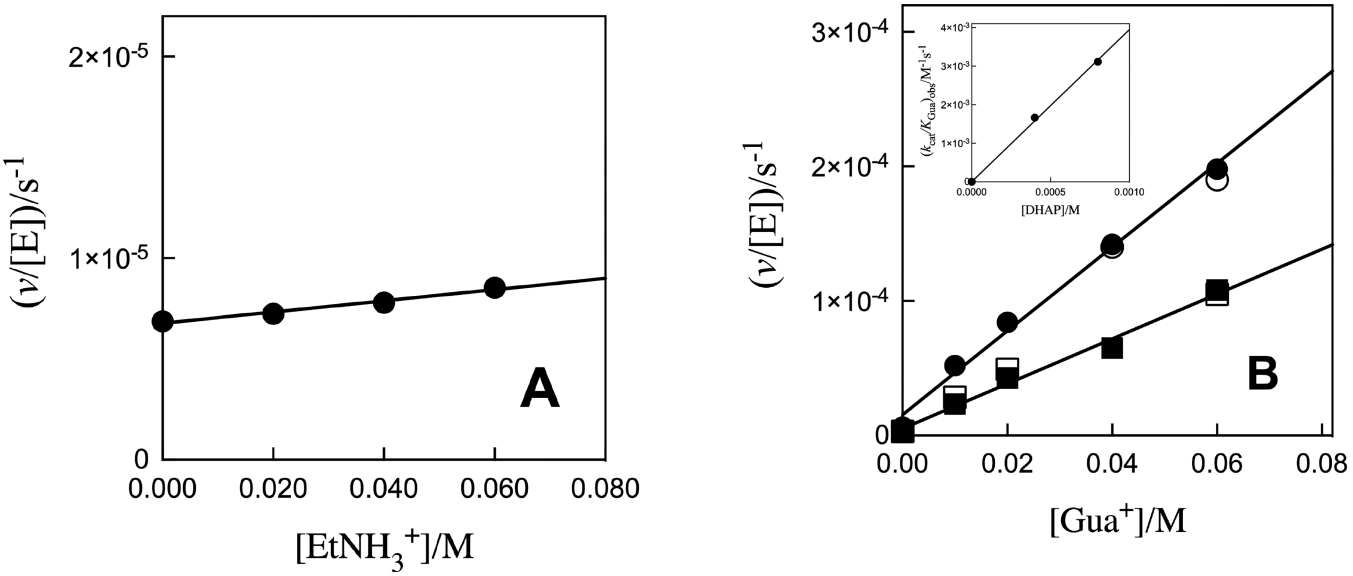

Figure 3. (A) Effect of increasing [$EtNH_3^+$] on $v/[E]$ (s^{-1}) for K120A/R269A variant *hl*GPDH-catalyzed reduction of 0.8 mM DHAP by saturating 0.2 mM NADH for reactions at pH 7.5 (20 mM TEA buffer), 25 °C, [NADH] = 0.2 mM, and I = 0.12 (NaCl). (B) Effect of increasing [Gua^+] on $v/[E]$ (s^{-1}) for K120A/R269A variant *hl*GPDH-catalyzed reduction of DHAP by 0.2 mM NADH for reactions at pH 7.5 (20 mM TEA buffer), 25 °C, saturating [NADH] = 0.2 mM, and I = 0.12 (NaCl): (●) 0.8 mM DHAP and (■) 0.4 mM DHAP. The inset shows the plot of $(k_{cat}/K_{Gua})_{obs}$ against [DHAP], where $(k_{cat}/K_{Gua})_{obs}$ values are the slopes of the correlations from the main panel. The empty symbols show the agreement of data obtained for two different preparations of the K120A/R269A variant.

Figure 4A ([DHAP] = 0.4 mM) and Figure 4B ([DHAP] = 0.8 mM) show plots of $v/[E]$ against [Gua^+], with slopes $(k_{cat}/K_{Gua})_{obs}$, for K120A/R269A *hl*GPDH-catalyzed reduction of DHAP by 0.2 mM NADH at different fixed concentrations of $EtNH_3^+$. Figure 5 shows plots of $(k_{cat}/K_{Gua})_{obs}$ from panels A and B of Figure 4 against [$EtNH_3^+$], with slopes $(k_{cat}/K_{Gua}K_{am})_{obs}$, for K120A/R269A *hl*GPDH-catalyzed reduction of 0.4 or 0.8 mM DHAP by 0.2 mM NADH. The inset of Figure 5 shows the plot of $(k_{cat}/K_{Gua}K_{am})_{obs}$ against [DHAP], with a slope $(k_{cat}/K_mK_{Gua}K_{am})$ of 1900 M^{-3} s^{-1} (Scheme 2 and Table 1).

DISCUSSION

The failure to detect reduction of GA catalyzed by 20 μM R269A *hl*GPDH results in a $(k_{cat}/K_m)_{obs}$ of ≤0.003 M^{-1} s^{-1} for the variant *hl*GPDH-catalyzed reaction.[3] The failure to observe activation of the reduction of GA catalyzed by 30 μM K120A/R269A *hl*GPDH by 20 mM HP_i, Gua^+, or $EtNH_3^+$ activators or by a mixture of 20 mM HP_i, 20 mM Gua^+, and 20 mM $EtNH_3^+$ shows that $(k_{cat}/K_m)_{obs} \leq 0.003$ M^{-1} s^{-1} for the K120A/R269A variant-catalyzed reaction in the presence of these activators. Equation 1 gives the relationship between this limit for $(k_{cat}/K_m)_{obs}$ and the fifth-order rate constant k_Q for the reaction catalyzed by the quaternary complex of the K120A/R269A variant, GA, HP_i, Gua^+, and $EtNH_3^+$. These data set an upper limit for k_Q of 375 M^{-4} s^{-1} (eq 2). This shows that two small molecules may act together to give detectable activation of GPDH under our experimental conditions [HP_i and Gua^+ for R269A variant *hl*GPDH-catalyzed reduction of GA[3] and Gua^+ and $EtNH_3^+$ for K120A/R269A variant *hl*GPDH-catalyzed reduction of DHAP (this work, Table 1)] but that it is not

https://dx.doi.org/10.1021/acs.biochem.0c00175
Biochemistry 2020, 59, 1582−1591

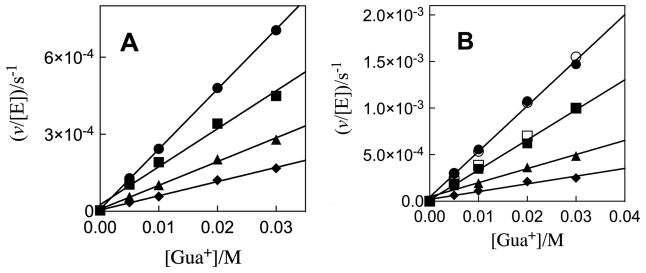

Figure 4. Effect of increasing $[Gua^+]$ and $[EtNH_3^+]$ on $v/[E]$ for K120A/R269A variant *hl*GPDH-catalyzed reduction of DHAP by NADH at pH 7.5 (20 mM TEA buffer), 25 °C, saturating [NADH] = 0.2 mM, and I = 0.12 (NaCl). (A) Increase in $v/[E]$, with increasing $[Gua^+]$, for the reaction of 0.4 mM DHAP at different fixed $EtNH_3^+$ concentrations. (B) Increase in $v/[E]$, with increasing $[Gua^+]$, for the reaction of 0.8 mM DHAP at different fixed $EtNH_3^+$ concentrations: (◆) 5 mM $EtNH_3^+$, (▲) 10 mM $EtNH_3^+$, (■) 20 mM $EtNH_3^+$, and (●) 30 mM $EtNH_3^+$. The empty symbols show the agreement of data obtained for two different preparations of the K120A/R269A variant *hl*GPDH.

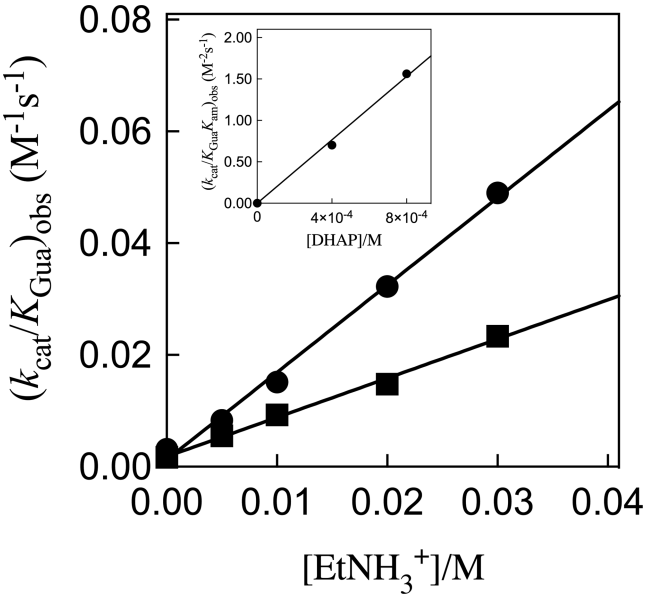

Figure 5. Effect of increasing $[EtNH_3^+]$ on $(k_{cat}/K_{Gua})_{obs}$ for K120A/R269A variant *hl*GPDH-catalyzed reduction of DHAP by NADH at pH 7.5 (20 mM TEA buffer), 25 °C, saturating [NADH] = 0.2 mM, and I = 0.12 (NaCl). The slope of these correlations is $(k_{cat}/K_{Gua}K_{am})_{obs}$ for variant *hl*GPDH-catalyzed reduction activated by the combined action of Gua^+ and $EtNH_3^+$: (■) 0.4 mM DHAP and (●) 0.8 mM DHAP. The inset shows the plot of $(k_{cat}/K_{Gua}K_{am})_{obs}$ against [DHAP], with a slope $(k_{cat}/K_mK_{Gua}K_{am})$ of 1900 M^{-3} s^{-1} (Scheme 2 and Table 1).

Scheme 2. Rescue of the K120A/R269A Variant *hl*GPDH by $EtNH_3$ and Gua^+

$$E{\bullet}NADH + DHAP \underset{Gua^+ + EtNH_3^+}{\overset{(k_{cat}/K_mK_{Gua}K_{am})}{\rightleftharpoons}} E{\bullet}NAD + Gly\text{-}3\text{-}P_i$$

possible to detect activation by the combined action of HP_i, Gua^+, and $EtNH_3^+$.

$$(k_{cat}/K_m)_{obs} = k_Q[Gua^+][HP_i][EtNH_3^+] = k_Q(8 \times 10^{-6}\ M^3) \leq 0.003\ M^{-1} \quad (1)$$

$$\frac{(k_{cat}/K_m)_{obs}}{[Gua^+][HP_i][EtNH_3^+]} = k_Q \leq \frac{0.003\ M^{-1}}{8 \times 10^{-6}\ M^3} \leq 375\ M^{-4}\ s^{-1} \quad (2)$$

Rescue of the K120A/Q295A Variant-Catalyzed Reactions of DHAP. The K120A substitution results in similar 5.3 and 6.2 kcal/mol increases in the activation barrier for wild type- and Q295A variant-catalyzed reduction of DHAP, respectively (Table 1).[21] The efficiency of rescue of the activity of the K120A/Q295A variant by $EtNH_3^+$ was characterized in this work (Figure 2) and compared with the efficiency of rescue of the K120A variant (Table 1).[21] The transition states for the K120A and K120A/Q295A *hl*GPDH-catalyzed reductions of DHAP show similar stabilizations of 3.0 and 3.6 kcal/mol, respectively, for reactions in the presence of 1.0 M $EtNH_3^+$, while the EMs of 50 and 70 M determined for the K120 side chain of the wild type and the Q295A variant of *hl*GPDH, respectively, are similar (Table 1). These data provide additional support for the conclusion that the Q295A substitution only slightly impairs the transition state stabilization by the K120 side chain.[21]

K120A/R269A Variant-Catalyzed Reactions of DHAP. The position of side chains at the ternary *hl*GPDH·NAD·DHAP complex is shown in Figure 1, while panels A–C of Figure 6 show the side chains as representations of the surface of the binary *hl*GPDH·NAD complex (Figure 6A), the binary *hl*GPDH·NAD complex with DHAP inserted at the position of the ternary complex (Figure 6B), and the ternary *hl*GPDH·NAD·DHAP complex (Figure 6C). The K120 and R269 side chains lie on opposite sides of the active site cavity, with the K120 side chain positioned to interact with the carbonyl group and the R269 side chain positioned to interact with the phosphodianion of the substrate. The side chains lie at the two ends of a network of highly conserved side chains (Figure 1), which extends from Q295 to K120 and includes R269, N270, N205, K204, D260, and K120. A comparison of the structures shown in panels A–C of Figure 6 shows that the ligand-driven enzyme conformational change results in the folding of a flexible protein loop (292-LNGQKL-297) over the DHAP and NAD cofactor that is facilitated by formation of a hydrogen bond between the Q295 and R269 side chains. Loop closure traps the substrate in a solvent-occluded cage, where the K120 and R269 side chains are optimally placed for catalysis, and where electrostatic catalysis is presumably enhanced by the decrease in the effective dielectric constant of the closed compared to the open form of the complex (Figure 6A–C).[29−31]

The consecutive K120 and R269 substitutions result in a total 12 kcal/mol increase in the activation barrier $\Delta G^{\ddagger}$ for hydride transfer (Scheme 3). The efficient rescue of the K120A/R269A variant of *hl*GPDH by Gua^+ and $EtNH_3^+$ (Figures 4 and 5) shows that the wild type and variant enzymes proceed through similar transition states, which are strongly stabilized by interactions with the K120 and R269 side chains (wild type *hl*GPDH) or with bound Gua^+ and $EtNH_3^+$. The larger sum of the effects of individual K120A and R269A substitutions on $\Delta G^{\ddagger}$ (5.3 + 9.1 = 14.4 kcal/mol) shows that the interaction energies of the single side chains of wild type *hl*GPDH are higher than the total 12 kcal/mol interaction determined by deleting the two side chains.

The 2.4 kcal/mol difference between the total side chain interaction estimated when the remaining side chain is preserved and the interaction determined by deleting both

https://dx.doi.org/10.1021/acs.biochem.0c00175
Biochemistry 2020, 59, 1582−1591

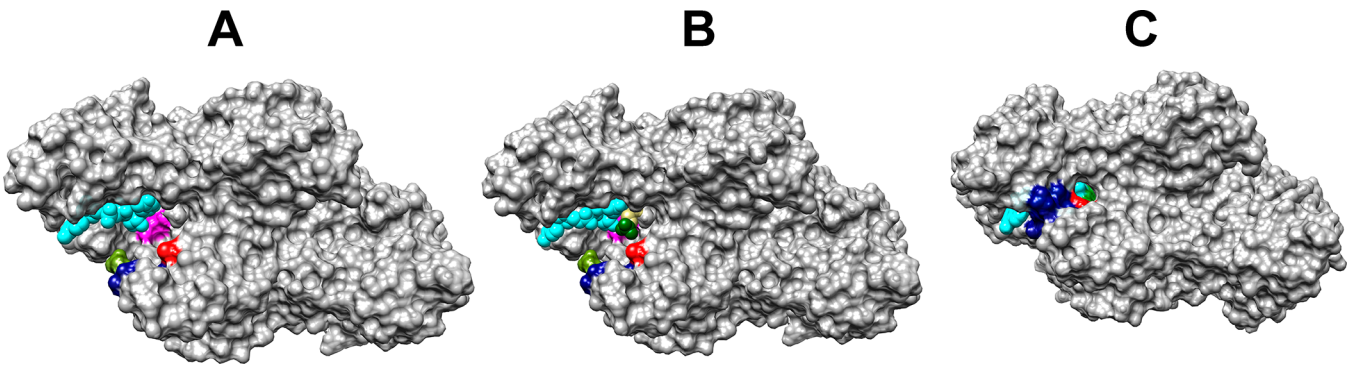

Figure 6. Representations of the protein surface for binary and ternary complexes of *hl*GPDH: (A) binary complex with NAD (PDB entry 6E8Z), (B) binary complex with NAD with substrate DHAP inserted at the position observed for the ternary *hl*GPDH·NAD·DHAP complex, and (C) ternary *hl*GPDH·NAD·DHAP complex (PDB entry 6E90). Color key: NAD, cyan; flexible protein loop (292-LNGQKL-297), navy blue; Q295, olive; R269, red; K120, magenta; DHAP, dark green for the phosphodianion and khaki for the remainder of the substrate. Substrate binding is accompanied by a movement of the navy blue flexible protein loop that covers the substrate and cofactor in the closed enzyme, formation of a hydrogen bond between the Q295 (olive) and R269 (red) side chains, and movement of the R269 side chain toward the substrate phosphodianion (green) and the cofactor pyrophosphate (cyan). The buried K120 side chain and substrate phosphodianion are hidden from view in panel C.

Scheme 3. Cycle That Shows the Effect of Consecutive K120A and R269A Substitutions on $\Delta\Delta G^{\ddagger}$ for Wild Type *hl*GPDH-Catalyzed Reduction of DHAP by NADH

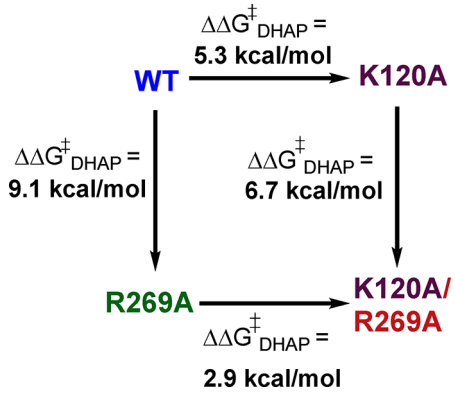

side chains (Scheme 3) represents the stronger side chain interactions of the tight, organized, conformation of wild type *hl*GPDH, compared to interactions of the K120A or R269A variant. We propose that this difference is due to effects of the first substitution, which reduce the transition state stabilization by the second side chain, such as an increase in the side chain conformational flexibility. This proposal is consistent with the notion that wild type *hl*GPDH derives a catalytic advantage from the high degree of organization of the catalytic side chains at the wild type active site and that the effect on $\Delta G^{\ddagger}$ of substitutions that erode this organization is greater than the effect of the lost interaction between the transition state and excised side chain.

Rescue of K120A/R269A *hl*GPDH by $EtNH_3^+$ and Gua^+. The kinetic data for rescue of the K120A/R269A variant of *hl*GPDH by Gua^+ and $EtNH_3^+$ give a $(\Delta\Delta G^{\ddagger}_{Act})_{EtNH_3\cdot Gua}$ of 7.5 kcal/mol (eq 3, Table 1) for stabilization of the transition state by interaction with the bound cations that is only 4.5 kcal/mol smaller than the transition state stabilization by the K120 and R269 side chains of wild type *hl*GPDH ($\Delta\Delta G^{\ddagger}$ = 12.0 kcal/mol, eq 4). The difference corresponds to a 12.0 − 7.5 = $(\Delta G^{\ddagger}_{S})_{E+EtNH_3+Gua}$ = 4.5 kcal/mol advantage to the reaction catalyzed by wild type *hl*GPDH compared to catalysis by the K120A/R269A variant in the presence of 1.0 M Gua^+ and $EtNH_3^+$ (eq 5). By comparison, the binding of 1.0 M $EtNH_3^+$ or 1.0 M Gua^+ to the K120A/R269A variant provides a $(\Delta G^{\ddagger}_{Act})_{EtNH_3}$ = 1.0 (eq 6) or $(\Delta G^{\ddagger}_{Act})_{Gua}$ = 3.8 kcal/mol (eq 7) stabilization, respectively, of the transition state for the reaction catalyzed by this variant, so that the sum of transition state stabilization by the individual cations in binary complexes (1.0 + 3.8 = 4.8 kcal/mol) is 2.7 kcal/mol smaller than the 7.5 kcal/mol stabilization observed for the cations in the ternary complex.

$$(\Delta\Delta G^{\ddagger}_{Act})_{EtNH_3\cdot Gua} = -RT\ln\left[\frac{k_{cat}/K_m K_{Gua} K_{EtNH_3}}{(k_{cat}/K_m)_{K120A/R269A}}\right] = -7.5\ \text{kcal/mol} \quad (3)$$

$$(\Delta\Delta G^{\ddagger}) = -RT\ln\left[\frac{(k_{cat}/K_m)_{WT}}{(k_{cat}/K_m)_{K120A/R269A}}\right] = -12.0\ \text{kcal/mol} \quad (4)$$

$$(\Delta G^{\ddagger}_{S})_{E+EtNH_3+Gua} = RT\ln\left[\frac{(k_{cat}/K_m)_{WT}}{k_{cat}/K_m K_{Gua} K_{EtNH_3}}\right] = 4.5\ \text{kcal/mol} \quad (5)$$

Scheme 4. Comparison between the Total Transition State Stabilization for Wild Type *hl*GPDH by Interactions with the K120 and R269 Side Chains and the Transition State Stabilization for the K120A/R269A Variant by Interactions with Exogenous Cations

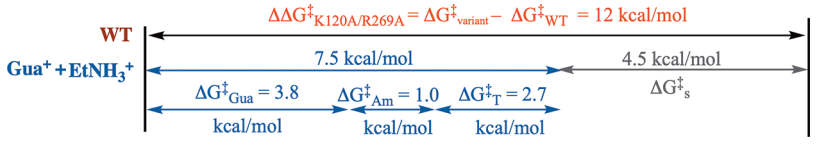

https://dx.doi.org/10.1021/acs.biochem.0c00175
Biochemistry 2020, 59, 1582−1591

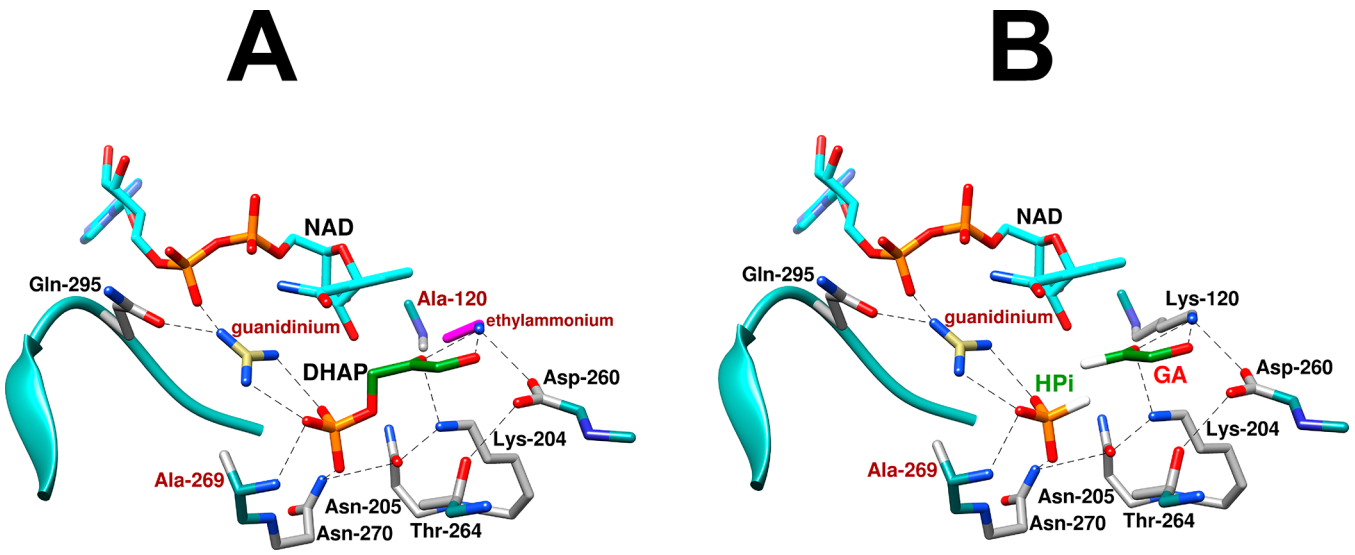

Figure 7. (A) Representations of the X-ray crystal structures of the following complexes with variant *hl*GPDH. (A) Complex of K120A/R269A *hl*GPDH with NAD, DHAP, Gua^+, and $EtNH_3^+$. (B) Complex of R269A *hl*GPDH with NAD, GA, HP_i, and Gua^+. The complexes were generated *in silico*, starting with Figure 1 for the X-ray crystal structure of the nonproductive complex of wild type *hl*GPDH, DHAP, and NAD^+ (PDB entry 6E90) with deletion of the relevant covalent linkage(s) while maintaining a fixed position for the remaining atoms of the hypothetical Michaelis complexes.

$$(\Delta G^{\ddagger}_{Act})_{EtNH_3} = -RT \ln\left[\frac{k_{cat}/K_m K_{EtNH_3}}{(k_{cat}/K_m)_{K120A/R269A}}\right] = -1.0 \text{ kcal/mol} \quad (6)$$

$$(\Delta G^{\ddagger}_{Act})_{Gua} = -RT \ln\left[\frac{k_{cat}/K_m K_{Gua}}{(k_{cat}/K_m)_{K120A/R269A}}\right] = -3.8 \text{ kcal/mol} \quad (7)$$

These results are illustrated by Scheme 4, which partitions the total 12.0 kcal/mol effect of the K120A and R269A substitutions on transition state stability into the 7.5 kcal/mol interaction recovered in the $EtNH_3^+ \cdot Gua^+$ complex and the 4.5 kcal/mol advantage to the reaction of the intact enzyme. The 7.5 kcal/mol recovered interaction is then partitioned into the 1.0 and 3.8 kcal/mol transition state stabilization of the individual binary complexes and the 2.7 kcal/mol advantage for cation activation of the ternary $E' \cdot EtNH_3^+ \cdot Gua^+$ complex. By comparison, the sum of the effect of single K120 and R269 substitutions in the K120A/R269A variant of *hl*GPDH (6.7 + 3.0 = 9.7 kcal/mol) on the stability of the transition state for enzyme-catalyzed reduction of DHAP is 2.3 kcal/mol smaller than the overall 12 kcal/mol stabilization by consecutive K120 and R269 substitutions (Scheme 3). We conclude that substitution of a single cationic side chain, or binding of a small molecule side chain analogue, in the K120A/R269A variant enhances the interaction of the second side chain or cation. We propose that this is due to utilization of the binding energy of the first bound cation in the organization of the active site, which enhances the transition state stabilization by the second bound cation. It is interesting that these cooperative interactions are expressed between side chains that are separated by ~9 Å.

The 4.5 kcal/mol "connection energy" (Scheme 4) is an estimate for the advantage to connecting the Gua^+ and $EtNH_3^+$ cations to the protein at the K120A/R269A variant of *hl*GPDH. This defines the effective concentration or effective molarity (EM)[11] of the side chains of wild type *hl*GPDH compared to the value of 1.0 M of the free side chain in water (Table 1). EMs of 50 and 60 M were determined for the K120 and R269 side chains from the efficiency of rescue of the K120A and R269A variants, respectively.[3,21] The product of the EMs from studies of single variants (50 M)(60 M) = 3000 M^2 is similar to the value of 2400 M^2 determined from rescue studies of the K120A/R269A variant (Table 1). This is consistent with similar stabilizing interactions between the catalyst and rescue agents of the K120A and R269A single variants and the K120A/R269A double variant.

The EMs from Table 1 are clustered between 30 and 140 M and correspond to an ~2.5 kcal/mol advantage in $\Delta G^{\ddagger}_S$ for reactions catalyzed by wild type *hl*GPDH compared to the reactions catalyzed by the complex between the variant enzyme and the missing piece. These values of EMs and $\Delta G^{\ddagger}_S$ are smaller than the values of ~10^6 M and ≈8 kcal/mol predicted for cases in which the advantage for unimolecular compared with bimolecular reaction is wholly entropic.[14,32] The low EMs from Table 1 reflect the effective stabilization of the complexes to the pieces by interactions with the protein catalyst (Figure 1),[15] where the K120 chain is locked into place by an ion pair to the D260 side chain,[21] and the R269 side chain is held by interactions with the phosphodianion of DHAP, the pyrophosphate anion of NAD, and the Q295 side chain (Figure 1). These same interactions stabilize the $EtNH_3^+$ and Gua^+ pieces bound to the K120A/R269A variant of *hl*GPDH (Figure 7A).

Efficiency of Hydride Transfer Catalyzed by *hl*GPDH. The large transition state stabilization for *hl*GPDH-catalyzed reduction of DHAP is achieved largely through strong, focused, stabilizing interactions with the K120 and R269 side chains.[21] The recovery of these interactions through the robust rescue of the K120A/R269A variant by Gua^+ and $EtNH_3^+$ enzyme pieces reflects the strong stabilization of complexes with Gua^+ and $EtNH_3^+$ (Figure 7A) by interaction with the neighboring amino acid side chains discussed above. Similarly, there is efficient activation of R269A variant *hl*GPDH-catalyzed reduction of glycolaldehyde by the combined action of the exogenous phosphite dianion and guanidine cation.[3] This is a

https://dx.doi.org/10.1021/acs.biochem.0c00175
Biochemistry 2020, 59, 1582−1591

consequence of the stabilization of the enzyme-bound HP_i·Gua^+ ion pair (Figure 7B) by hydrogen bonding and ionic interactions, respectively, of Gua^+ with the Q295 side chain and the cofactor pyrophosphate oxygen and by hydrogen bonds between HP_i and the A269 backbone amide and the N270 amide side chain.

The side chain interactions, which promote efficient rescue of the K120A and R269A variants, serve to organize (or to preorganize)[33−35] the K120 and R269 side chain cations of wild type *hl*GPDH (Figure 1). We propose that this preorganization enables the large, focused, 12 kcal/mol transition state stabilization from interactions with the K120 and R269 side chains by minimizing the energetic price for side chain immobilization that occurs on proceeding from the Michaelis complex to the hydride transfer transition state.[30] Additional examples of side chain preorganization at enzyme active sites, such as the catalytic triad found in serine proteases,[36,37] have been discussed by Warshel and co-workers.[34,35,38−40]

There are surprising similarities between the mechanisms for hydride transfer from NADH to DHAP catalyzed by *hl*GPDH and for isomerization of DHAP, with proton transfer, catalyzed by triosephosphate isomerase (TIM). Each enzyme shows strong phosphite dianion (HP_i) activation of catalysis of the reaction of the common truncated substrate glycolaldehyde. The K12 side chain at TIM sits near the substrate dianion, and the K12G variant shows efficient rescue by alkyl ammonium cations. However, there is no rescue of K12G-catalyzed deprotonation of GA by the combined action of HP_i and RNH_3^+. The stronger stabilization of the transition state for R269A variant-catalyzed hydride transfer to GA by the HP_i·Gua^+ ion pair compared with the transition state for K12G variant-catalyzed deprotonation of GA by the HP_i·$EtNH_3^+$ ion pair is consistent with a higher degree of preorganization of the ion pair at the active site of *hl*GPDH. This reflects, at least in part, the presence of an intervening water molecule between the substrate phosphodianion and the TIM K12 side chain.

A Conserved Network of Amino Acid Side Chains. The highly conserved side chains from Q295, R269, N270, N205, T264, K204, D260, and K120 form a continuous chain of hydrogen bonds that stretch from the bound cofactor to the carbonyl group of DHAP (Figures 1 and 7).[24,25] This side chain conservation suggests that the network operates as a unit, with K120, K204, and R269 providing direct transition state stabilization; N205, D260, and Q295 functioning directly to immobilize the catalytic side chains; and N270, N205, and T264 playing secondary roles in maintaining the network's structural integrity. We suggest that this tight network of side chain interactions promotes effective catalysis and that the preorganization of this network by intra-side chain interactions with K120 and R269 provides a mechanism for the expression of cooperative interactions between the two cations, which are separated by 9 Å (Figure 1).

The D260 side chain shows no direct stabilizing interaction with the hydride transfer transition state, and there should be only a weak interaction with the N270 side chain. The large 6.5 and 5.6 kcal/mol effects of D260G[21] and N270A[25] substitutions, respectively, on the stability of the transition state for wild type *hl*GPDH-catalyzed reduction of DHAP by NADH (neither of which is subject to small molecule rescue) are therefore consistent with a substantial reorganization of the extended side chain network at the D260G and N270A variants, which results in barriers to formation of the preorganized, catalytically active closed conformation of variant *hl*GPDH. Finally, the observation that the N270A substitution results in an ∼40-fold increase in k_{cat}/K_m for enzyme-catalyzed reduction of GA by NADH is consistent with a reorganization of the active site at this variant, which favors binding of GA in a reactive conformation. This unusual observation shows that there is still much to be learned about the exact role of this extended network of interactions in the organization of active site side chains that provides for optimal catalysis of the reactions of whole and truncated substrates.

CONCLUSIONS

The R269 side chain of GPDH functions to trap the substrate DHAP in a tight cage,[16,29] which provides strong stabilization of the transition state for hydride transfer, while the K120 side chain acts to stabilize negative charge at the C-2 oxygen, which develops in this transition state.[21] The K120A and R269A substitutions at GPDH result in a total 7×10^8-fold decrease in k_{cat}/K_m for reduction of DHAP by NADH, which corresponds to an enormous 12 kcal/mol destabilization of the transition state for hydride transfer: the K120A/R269A variant provides an excellent template for association of exogenous Gua^+ and $EtNH_3^+$ activators, which afford a 7.5 kcal/mol transition state stabilization at standard states of 1.0 M Gua^+ and $EtNH_3^+$. The transition state stabilization from single R269 or K120 side chains, or from single Gua^+ or $EtNH_3^+$ activators, is enhanced by the presence of the second side chain or activator. These results provide compelling support for the conclusion that the network of conserved side chains at GPDH (Figure 1) functions in the preorganization of the K120 and R269 side chains into positions that provide optimal stabilization of the transition state for hydride transfer. This preorganization promotes cooperativity in the expression of the strongly stabilizing interactions of the K120 and R269 side chains across a separation distance of 9 Å. We propose that the side chains at enzyme active sites often function organically and as a unit to provide for optimal stabilizing interactions between the transition state and a few key catalytic side chains.

ASSOCIATED CONTENT

Accession Codes

Human glycerol-3-phosphate dehydrogenase [NAD^+], cytoplasmic, UniProt accession code P21695.

AUTHOR INFORMATION

Corresponding Author

John P. Richard − *Department of Chemistry, University at Buffalo, State University of New York, Buffalo, New York 14260-3000, United States;* orcid.org/0000-0002-0440-2387; Email: jrichard@buffalo.edu

Authors

Judith R. Cristobal − *Department of Chemistry, University at Buffalo, State University of New York, Buffalo, New York 14260-3000, United States*

Archie C. Reyes − *Department of Chemistry, University at Buffalo, State University of New York, Buffalo, New York 14260-3000, United States;* orcid.org/0000-0001-9955-393X

Complete contact information is available at: https://pubs.acs.org/10.1021/acs.biochem.0c00175

https://dx.doi.org/10.1021/acs.biochem.0c00175
Biochemistry 2020, 59, 1582−1591

Funding

The authors acknowledge National Institutes of Health Grants GM116921 and GM134881 for generous support of this work.

Notes

The authors declare no competing financial interest.

■ ABBREVIATIONS

*Sc*OMPDC, orotidine 5′-monophosphate decarboxylase from yeast; TIM, triosephosphate isomerase; GPDH, glycerol-3-phosphate dehydrogenase; *hl*GPDH, glycerol-3-phosphate dehydrogenase from human liver; DHAP, dihydroxyacetone phosphate; etG, ethylene glycol; GA, glycolaldehyde; NADH, nicotinamide adenine dinucleotide, reduced form; NAD, nicotinamide adenine dinucleotide, oxidized form; MES, 2-(*N*-morpholino)ethanesulfonic acid; TEA, triethanolamine; DTT, D,L-dithiothreitol; BSA, bovine serum albumin.

■ REFERENCES

(1) Peracchi, A. (2008) How (and why?) to revive a dead enzyme: The power of chemical rescue. *Curr. Chem. Biol. 2*, 32−49.
(2) Olucha, J., Meneely, K. M., and Lamb, A. L. (2012) Modification of Residue 42 of the Active Site Loop with a Lysine-Mimetic Side Chain Rescues Isochorismate-Pyruvate Lyase Activity in Pseudomonas aeruginosa PchB. *Biochemistry 51*, 7525−7532.
(3) Reyes, A. C., Amyes, T. L., and Richard, J. P. (2016) Enzyme Architecture: Self-Assembly of Enzyme and Substrate Pieces of Glycerol-3-Phosphate Dehydrogenase into a Robust Catalyst of Hydride Transfer. *J. Am. Chem. Soc. 138*, 15251−15259.
(4) Reyes, A. C., Zhai, X., Morgan, K. T., Reinhardt, C. J., Amyes, T. L., and Richard, J. P. (2015) The Activating Oxydianion Binding Domain for Enzyme-Catalyzed Proton Transfer, Hydride Transfer and Decarboxylation: Specificity and Enzyme Architecture. *J. Am. Chem. Soc. 137*, 1372−1382.
(5) Tsang, W.-Y., Amyes, T. L., and Richard, J. P. (2008) A Substrate in Pieces: Allosteric Activation of Glycerol 3-Phosphate Dehydrogenase (NAD^+) by Phosphite Dianion. *Biochemistry 47*, 4575−4582.
(6) Amyes, T. L., and Richard, J. P. (2007) Enzymatic catalysis of proton transfer at carbon: activation of triosephosphate isomerase by phosphite dianion. *Biochemistry 46*, 5841−5854.
(7) Amyes, T. L., Richard, J. P., and Tait, J. J. (2005) Activation of orotidine 5′-monophosphate decarboxylase by phosphite dianion: The whole substrate is the sum of two parts. *J. Am. Chem. Soc. 127*, 15708−15709.
(8) Toney, M. D., and Kirsch, J. F. (1989) Directed Bronsted analysis of the restoration of activity to a mutant enzyme by exogenous amines. *Science 243*, 1485−1488.
(9) Hung, J. E., Fogle, E. J., Garg, N., Chekan, J. R., Nair, S. K., and van der Donk, W. A. (2014) Chemical Rescue and Inhibition Studies to Determine the Role of Arg301 in Phosphite Dehydrogenase. *PLoS One 9*, e87134−e87139.
(10) Lamba, V., Yabukarski, F., and Herschlag, D. (2017) An Activator−Blocker Pair Provides a Controllable On−Off Switch for a Ketosteroid Isomerase Active Site Mutant. *J. Am. Chem. Soc. 139*, 11089−11095.
(11) Kirby, A. (1980) Effective Molarities for Intramolecular Reactions. *Adv. Phys. Org. Chem. 17*, 183−278.
(12) Barnett, S. A., Amyes, T. L., McKay Wood, B., Gerlt, J. A., and Richard, J. P. (2010) Activation of R235A Mutant Orotidine 5′-Monophosphate Decarboxylase by the Guanidinium Cation: Effective Molarity of the Cationic Side Chain of Arg-235. *Biochemistry 49*, 824−826.
(13) Jencks, W. P. (1981) On the attribution and additivity of binding energies. *Proc. Natl. Acad. Sci. U. S. A. 78*, 4046−4050.
(14) Page, M. I., and Jencks, W. P. (1971) Entropic contributions to rate accelerations in enzymic and intramolecular reactions and the chelate effect. *Proc. Natl. Acad. Sci. U. S. A. 68*, 1678−1683.
(15) Go, M. K., Amyes, T. L., and Richard, J. P. (2010) Rescue of K12G mutant TIM by NH_4^+ and alkylammonium cations: The reaction of an enzyme in pieces. *J. Am. Chem. Soc. 132*, 13525−13532.
(16) Reyes, A. C., Koudelka, A. P., Amyes, T. L., and Richard, J. P. (2015) Enzyme Architecture: Optimization of Transition State Stabilization from a Cation−Phosphodianion Pair. *J. Am. Chem. Soc. 137*, 5312−5315.
(17) Bentley, P., and Dickinson, F. M. (1974) Coenzyme-binding characteristics of rabbit muscle L-glycerol 3-phosphate dehydrogenase. *Biochem. J. 143*, 11−17.
(18) Bentley, P., Dickinson, F. M., and Jones, I. G. (1973) Purification and properties of rabbit muscle L-glycerol 3-phosphate dehydrogenase. *Biochem. J. 135*, 853−859.
(19) Fondy, T. P., Ross, C. R., and Sollohub, S. J. (1969) Structural studies on rabbit muscle glycerol 3-phosphate dehydrogenase and a comparison of chemical and physical determinations of its molecular weight. *J. Biol. Chem. 244*, 1631−1644.
(20) Fondy, T. P., Levin, L., Sollohub, S. J., and Ross, C. R. (1968) Structure of L-glycerol-3-phosphate:NAD oxidoreductase isolated from rat skeletal muscle. *J. Biol. Chem. 243*, 3148−3160.
(21) Mydy, L. S., Cristobal, J., Katigbak, R., Bauer, P., Reyes, A. C., Kamerlin, S. C. L., Richard, J. P., and Gulick, A. M. (2019) Human Glycerol 3-Phosphate Dehydrogenase: X-Ray Crystal Structures that Guide the Interpretation of Mutagenesis Studies. *Biochemistry 58*, 1061−1073.
(22) Tsukiji, S., Pattnaik, S. B., and Suga, H. (2004) Reduction of an Aldehyde by a NADH/Zn 2+-Dependent Redox Active Ribozyme. *J. Am. Chem. Soc. 126*, 5044−5045.
(23) Choe, J., Guerra, D., MICHELS, P. A. M., and Hol, W. G. J. (2003) Leishmania mexicana glycerol-3-phosphate dehydrogenase showed conformational changes upon binding a bi-substrate adduct. *J. Mol. Biol. 329*, 335−349.
(24) Ou, X., Ji, C., Han, X., Zhao, X., Li, X., Mao, Y., Wong, L.-L., Bartlam, M., and Rao, Z. (2006) Crystal structures of human glycerol 3-phosphate dehydrogenase 1 (GPD1). *J. Mol. Biol. 357*, 858−869.
(25) Reyes, A. C., Amyes, T. L., and Richard, J. P. (2016) Enzyme Architecture: A Startling Role for Asn270 in Glycerol 3-Phosphate Dehydrogenase-Catalyzed Hydride Transfer. *Biochemistry 55*, 1429−1432.
(26) Gasteiger, E., Hoogland, C., Gattiker, A., Duvaud, A., Wilkins, M. R., Appel, R. D., and Bairoch, A. (2005) Protein Identification and Analysis Tools on the ExPASy Server. *Proteomics Protocols Handbook*, 571−607.
(27) Gasteiger, E., Gattiker, A., Hoogland, C., Ivanyi, I., Appel, R. D., and Bairoch, A. (2003) ExPASy: The proteomics server for in-depth protein knowledge and analysis. *Nucleic Acids Res. 31*, 3784−3788.
(28) He, R., Reyes, A. C., Amyes, T. L., and Richard, J. P. (2018) Enzyme Architecture: The Role of a Flexible Loop in Activation of Glycerol-3-phosphate Dehydrogenase for Catalysis of Hydride Transfer. *Biochemistry 57*, 3227−3236.
(29) Richard, J. P., Amyes, T. L., Goryanova, B., and Zhai, X. (2014) Enzyme architecture: on the importance of being in a protein cage. *Curr. Opin. Chem. Biol. 21*, 1−10.
(30) Richard, J. P. (2019) Protein Flexibility and Stiffness Enable Efficient Enzymatic Catalysis. *J. Am. Chem. Soc. 141*, 3320−3331.
(31) Amyes, T. L., Malabanan, M. M., Zhai, X., Reyes, A. C., and Richard, J. P. (2017) Enzyme activation through the utilization of intrinsic dianion binding energy. *Protein Eng., Des. Sel. 30*, 159−168.
(32) Jencks, W. P. (2006) Binding energy, specificity, and enzymic catalysis: the Circe effect. *Adv. Enzymol. Relat. Areas Mol. Biol. 43*, 219−410.
(33) Jindal, G., and Warshel, A. (2017) Misunderstanding the preorganization concept can lead to confusions about the origin of enzyme catalysis. *Proteins: Struct., Funct., Genet. 85*, 2157−2161.
(34) Warshel, A., Sharma, P. K., Kato, M., and Parson, W. W. (2006) Modeling electrostatic effects in proteins. *Biochim. Biophys. Acta, Proteins Proteomics 1764*, 1647−1676.

https://dx.doi.org/10.1021/acs.biochem.0c00175
Biochemistry 2020, 59, 1582−1591

(35) Warshel, A. (1998) Electrostatic Origin of the Catalytic Power of Enzymes and the Role of Preorganized Active Sites. *J. Biol. Chem. 273*, 27035−27038.
(36) Blankenship, E., Vukoti, K., Miyagi, M., and Lodowski, D. T. (2014) Conformational flexibility in the catalytic triad revealed by the high-resolution crystal structure of Streptomyces erythraeus trypsin in an unliganded state. *Acta Crystallogr., Sect. D: Biol. Crystallogr. 70*, 833−840.
(37) Hedstrom, L. (2002) Serine Protease Mechanism and Specificity. *Chem. Rev. 102*, 4501−4524.
(38) Kamerlin, S. C. L., Sharma, P. K., Chu, Z. T., and Warshel, A. (2010) Ketosteroid isomerase provides further support for the idea that enzymes work by electrostatic preorganization. *Proc. Natl. Acad. Sci. U. S. A. 107*, 4075−4080.
(39) Kamerlin, S. C. L., Chu, Z. T., and Warshel, A. (2010) On catalytic preorganization in oxyanion holes: highlighting the problems with the gas-phase modeling of oxyanion holes and illustrating the need for complete enzyme models. *J. Org. Chem. 75*, 6391−6401.
(40) Warshel, A., Sharma, P. K., Kato, M., Xiang, Y., Liu, H., and Olsson, M. H. M. (2006) Electrostatic basis for enzyme catalysis. *Chem. Rev. 106*, 3210−3235.

https://dx.doi.org/10.1021/acs.biochem.0c00175
Biochemistry 2020, 59, 1582−1591